

ALBERT-LUDWIGS-UNIVERSITÄT FREIBURG

Term Paper

---

# The Nobel Prize in Physics 2012

---



*Author:*  
Fabian Thielemann

*Supervisor:*  
Prof. Dr. Marcel Mudrich

*Submitted:*  
August 2, 2016

# Contents

<b>1</b>	<b>Introduction</b>	<b>2</b>
<b>2</b>	<b>Theory</b>	<b>3</b>
2.1	Jaynes-Cummings Hamiltonian . . . . .	3
2.2	Rabi Oscillations . . . . .	4
2.3	Dressed States . . . . .	5
2.4	Far Off Resonance Case . . . . .	6
<b>3</b>	<b>Serge Haroche</b>	<b>8</b>
3.1	Early Life and Scientific Career . . . . .	8
3.2	Quantum Beats . . . . .	9
3.3	Cavity Quantum Electrodynamics . . . . .	11
3.3.1	Enhanced Spontaneous Emission . . . . .	11
3.3.2	Suppressed Spontaneous Emission . . . . .	13
3.3.3	Quantum Non Demolition Measurement of Photons . . . . .	15
<b>4</b>	<b>David Wineland</b>	<b>18</b>
4.1	Early Life and Scientific Career . . . . .	18
4.2	Doppler Cooling . . . . .	19
4.3	Trapping Single Ions . . . . .	21
4.4	Ion Quantum Jumps . . . . .	22
4.5	Sideband Cooling . . . . .	23
4.6	Quantum Logic Gate . . . . .	24
<b>5</b>	<b>Conclusion</b>	<b>28</b>

## 1 Introduction

The Nobel prize in physics 2012 was awarded jointly to the French physicist Serge Haroche and the American physicist David Wineland. According to the Nobel jury they received it “for ground-breaking experimental methods that enable measuring and manipulation of individual quantum systems”. Serge Haroche spent most of his life researching at the École Normale Supérieure in Paris. There he created photon traps, i.e. cavities, in which microwave photons could be stored up to half a second [1]. To probe the wave function of the photons, he sent in groups of or single atoms to see how they would interact with the light. In this way he unveiled many of the interesting effects of the quantum nature of light. David Wineland spent most of his scientific life on the other side of the Atlantic, at the National Institute of Standards and Technology in Boulder, Colorado. His drive was to invent better methods to slow down and isolate ions as this allowed frequency measurements of higher and higher precision. To achieve this, he used sophisticated setups combining ion traps with high precision lasers.

But if one of the laureates dedicated his research to photons and the other one to ions, why did they share the Nobel prize? The answer to this question lies in the congruence of their methods with respect to quantum mechanics. Haroche was probing photons with atoms, Wineland examined the energy levels of atoms using photons, but both were dealing with the same underlying effects of quantum mechanics. This can be easily seen when one leaves aside their specific physical objects of study (i.e. photons and ions) and inspects which abstract topics they were dealing with. Both of them published papers about “Schrödinger Cat States” [2, 3], bringing to physical experiment one of the most fundamental thought experiments of early quantum mechanics. Both conducted experiments on many particle entanglement [4, 5]. Both found ways to engineer explicitly non-classical states in their systems [6, 7]. This list could be continued, but the message is clear: each of them in their own fields found ways to answer fundamental issues of quantum mechanics experimentally and on their way introduced countless new methods to the physics community.

The outline of this term paper is as follows: first we will theoretically derive the phenomenon of Rabi oscillations from the Jaynes-Cummings Hamiltonian, because both, Haroche and Wineland, used it as a central method in their later experiments (Sec. 2). Then we will have a look at each of the laureate’s early life and inspect some of their central experiments in order to get an impression of their experimental creativity and innovation (Sec. 3 and 4). A short conclusion will then be given in Sec. 5.

## 2 Theory

Some theoretical concepts of quantum optics are necessary to understand the ways in which Serge Haroche and David Wineland experimentally observed fundamental quantum mechanical effects. This section aims to introduce the basic model of a fully quantum mechanical description of atom-light interaction, the Jaynes-Cummings model, and one of the most frequently appearing consequences of it, Rabi oscillations.

### 2.1 Jaynes-Cummings Hamiltonian

Both, Serge Haroche and David Wineland, investigated and made use of the shifts in energy levels and relative phases of states that appear when a laser shines in on an atom. In order to give a useful and complete description of the interaction of atoms with light, one has to take into account that the energy levels of the atom and of the photon field are both quantized. The first “fully quantized” approach for the case of coherent light in a cavity and a two level system was given by Edwin Jaynes and Fred Cummings in 1963 [8]. To describe the system (following [9]) we introduce the total Hamiltonian, consisting of the Hamiltonian for the quantized photon field for a single mode, the Hamiltonian of the two level system consisting of a ground state  $|g\rangle$  and an excited state  $|e\rangle$  and the interaction Hamiltonian

$$\hat{H} = \hat{H}_{\text{field}} + \hat{H}_{\text{atom}} + \hat{H}_{\text{int}}, \quad (2.1)$$

where, neglecting the zero point energies of field and atom,

$$\hat{H}_{\text{field}} = \hbar\omega_f \hat{a}^\dagger \hat{a} \quad (2.2)$$

$$\hat{H}_{\text{atom}} = \frac{\hbar\omega_a}{2} \hat{\sigma}_3 \quad (2.3)$$

$$\hat{H}_{\text{int}} = \hbar\omega_{\text{int}} (\hat{\sigma}_+ + \hat{\sigma}_-) (\hat{a} + \hat{a}^\dagger). \quad (2.4)$$

Here  $\hat{a}^\dagger$  and  $\hat{a}$  are the creation and annihilation operators that appear in the quantization of the electromagnetic field<sup>1</sup>, the Pauli matrix  $\hat{\sigma}_3 = |e\rangle\langle e| - |g\rangle\langle g|$  acts as the inversion operator of the atom, and the associated Pauli matrices  $\hat{\sigma}_+ = |e\rangle\langle g|$  and  $\hat{\sigma}_- = |g\rangle\langle e|$  project any state  $|g\rangle$  ( $|e\rangle$ ) to  $|e\rangle$  ( $|g\rangle$ ) respectively and can thus be seen as atomic transition operators. It is now useful to look at the time evolution of the terms in the total Hamiltonian (2.1). To do so we switch to the interaction picture, using the Hamiltonian without interaction  $\hat{H}_0 = \hat{H}_{\text{atom}} + \hat{H}_{\text{field}}$  to describe the time evolution of the operators. For the annihilation operator we have

$$\hat{a}(t) = e^{i\hat{H}_0 t/\hbar} \hat{a}(0) e^{-i\hat{H}_0 t/\hbar}$$

---

<sup>1</sup>To solve the free field equation of the electromagnetic field one usually uses the Fourier ansatz

$$A^\mu(x) = \int d\vec{k} \sum_{\lambda=0}^3 \left[ a_\lambda(\vec{k}) \epsilon_\lambda^\mu(k) e^{-ikx} + a_\lambda^\dagger(\vec{k}) \epsilon_\lambda^\mu(k)^* e^{+ikx} \right],$$

where  $\lambda$  goes over all possible polarizations. When demanding that  $A^\mu$  and its conjugate field  $\pi^\nu$  obey the canonical quantization relation, the resulting commutator relations for  $a_\lambda$  and  $a_\lambda^\dagger$  allow the interpretation as creation and annihilation operators.

using the Baker-Campbell-Hausdorff formula, we obtain

$$= \hat{a}(0) + \frac{it}{\hbar} [\hat{H}_0, \hat{a}] + \frac{1}{2!} \left( \frac{it}{\hbar} \right)^2 [\hat{H}_0, [\hat{H}_0, \hat{a}]] + \dots$$

The first commutator is  $[\hat{H}_0, \hat{a}] = -\hbar\omega_f \hat{a}$  as  $\hat{a}$  commutes with  $\hat{H}_{\text{atom}}$  and  $[\hat{a}^\dagger, \hat{a}] = -1$ . The nested commutators will thus only add higher orders of  $\omega_f$ . The time evolution then becomes

$$\begin{aligned} &= \hat{a}(0) (1 - it\omega_f + (it\omega_f)^2 + \dots) \\ &= \hat{a}(0) e^{-i\omega_f t}. \end{aligned} \quad (2.5)$$

Correspondingly we obtain for the other operators

$$\hat{a}^\dagger(t) = \hat{a}^\dagger(0) e^{i\omega_f t} \quad (2.6)$$

$$\hat{\sigma}_\pm(t) = \hat{\sigma}_\pm(0) e^{\pm i\omega_a t} \quad (2.7)$$

and therefore the full interaction Hamiltonian becomes

$$\begin{aligned} \hat{H}_{\text{int}}(t) &= \hbar\omega_{\text{int}} (\hat{\sigma}_+ \hat{a} e^{i(\omega_a - \omega_f)t} + \hat{\sigma}_+ \hat{a}^\dagger e^{i(\omega_a + \omega_f)t} \\ &\quad + \hat{\sigma}_- \hat{a} e^{-i(\omega_a + \omega_f)t} + \hat{\sigma}_- \hat{a}^\dagger e^{-i(\omega_a - \omega_f)t}). \end{aligned} \quad (2.8)$$

Assuming that the photon frequency  $\omega_f$  is close to the transition frequency of the atom  $\omega_a$ , i.e.  $|\omega_a - \omega_f| \ll \omega_a + \omega_f$ , the rotating wave approximation can be applied. This means that all terms in  $\hat{H}_{\text{int}}$  that oscillate with  $\omega_a + \omega_f$  are neglected. Doing this and transforming back to the Schrödinger picture leaves us with the total Hamiltonian

$$\hat{H}_{\text{tot}} = \hbar\omega_f \hat{a}^\dagger \hat{a} + \frac{\hbar\omega_a}{2} \hat{\sigma}_3 + \hbar\omega_{\text{int}} (\hat{\sigma}_+ \hat{a} + \hat{\sigma}_- \hat{a}^\dagger). \quad (2.9)$$

The last two terms can be seen as processes in which the atom absorbs or emits one photon from the field while respectively changing its internal energy state.

## 2.2 Rabi Oscillations

Having found a Hamiltonian that describes the interaction of an atom with light, it is now interesting to investigate how this interaction influences the dynamics of the system. The original states of atom and field will no longer be eigenstates of the system and thus undergo a continuous oscillation, called Rabi oscillation. Both Serge Haroche and David Wineland made experimental use of this effect in order to prepare and manipulate states. To describe the dynamics it is first useful to split the Hamiltonian in (2.9) into two parts, namely

$$\hat{H}_I = \underbrace{\hbar\omega_f (\hat{a}^\dagger \hat{a} + |e\rangle \langle e|)}_{\text{excitation number } \hat{N}_e} + \hbar \left( \frac{\omega_a}{2} - \omega_f \right) \underbrace{(|e\rangle \langle e| + |g\rangle \langle g|)}_{\text{e}^- \text{ number projector } \hat{P}_e} \quad (2.10)$$

$$\hat{H}_{II} = -\hbar \underbrace{(\omega_a - \omega_f)}_{\equiv \Delta} |g\rangle \langle g| + \hbar\omega_{\text{int}} (\hat{\sigma}_+ \hat{a} + \hat{\sigma}_- \hat{a}^\dagger). \quad (2.11)$$

---

<sup>2</sup>By looking at the preceding footnote and considering that  $kx$  is a scalar product of four-vectors but the integration over  $d\tilde{k}$  is only over the three spatial components, we see that the time evolution behavior is already built-in in this ansatz.

The first part  $\hat{H}_I$  commutes with  $\hat{H}_{\text{tot}}$  thus it is conserved over time and any interesting dynamics of the system are described by the second part. Let us now consider a state

$$|\psi(t)\rangle = C_1(t)|e\rangle|n\rangle + C_2(t)|g\rangle|n+1\rangle \quad (2.12)$$

with initial conditions  $C_1(0) = 1$  and  $C_2(0) = 0$ . The time evolution is described by the time dependent Schrödinger equation  $i\hbar\frac{d}{dt}|\psi(t)\rangle = \hat{H}_{II}|\psi(t)\rangle$ . In the resonant case ( $\Delta = 0$ ) this can be exactly solved and yields

$$C_1(t) = \cos(\omega_{\text{int}}\sqrt{n+1}t) \quad (2.13)$$

$$C_2(t) = -i \sin(\omega_{\text{int}}\sqrt{n+1}t) \quad (2.14)$$

We see that the state of a two level system can be manipulated by sending in coherent light, a technique that is crucial for many quantum optics experiments. In this context a nomenclature for pulses is established, describing to what extent the light interacts with the atom. A pulse of light is called “ $r\pi$ -pulse” ( $r \in \mathbb{R}$ ) if it interacts with an atom such that

$$\omega_{\text{int}}\sqrt{n+1}t = \frac{r\pi}{2}. \quad (2.15)$$

A commonly used type of pulse is for example the  $\pi/2$ -pulse that takes e.g. a pure state  $|e\rangle|n\rangle$  to a superposition state  $\frac{1}{\sqrt{2}}(|e\rangle|n\rangle - i|g\rangle|n+1\rangle)$ . In the basis spanned by  $\{|e\rangle|n\rangle, |g\rangle|n+1\rangle\}$  a  $\pi/2$ -pulse can be represented in matrix form as

$$U(\pi/2) = \frac{1}{\sqrt{2}} \begin{pmatrix} 1 & -i \\ -i & 1 \end{pmatrix}. \quad (2.16)$$

The repeated action of a  $\pi/2$ -pulse on a two level system is shown graphically in Fig. 2.1. It should be noted that starting from  $|e\rangle|n\rangle$  and performing a full Rabi cycle will introduce a global phase of  $-1$  to the system. However this phase is not of physical importance when the two level system is closed and only measurable in comparison to a reference system.<sup>3</sup>

## 2.3 Dressed States

Description of the dynamics of a two level system in the off-resonant case requires diagonalization of the Hamiltonian (2.9). The resulting eigenstates are called “dressed states”, a wording that suggests that they are atom states “dressed in light” in contrast to the “bare” states of the atom without a light field. Using again the basis  $\{|e\rangle|n\rangle, |g\rangle|n+1\rangle\}$  we can represent (2.9) as

$$\hat{H}_{\text{tot}} = \begin{pmatrix} n\omega_f + \frac{1}{2}\hbar\omega_a & \hbar\omega_{\text{int}}\sqrt{n+1} \\ \hbar\omega_{\text{int}}\sqrt{n+1} & (n+1)\omega_f - \frac{1}{2}\omega_a \end{pmatrix} \quad (2.17)$$

and diagonalize it. From this we obtain the eigenenergies

$$E_{\pm} = \hbar\omega_f \left( n + \frac{1}{2} \right) \pm \hbar\Omega_n(\Delta) \quad (2.18)$$

---

<sup>3</sup> $\langle e|\hat{O}|e\rangle = \langle e|(-1)\hat{O}(-1)|e\rangle$  for any observable  $\hat{O}$ .

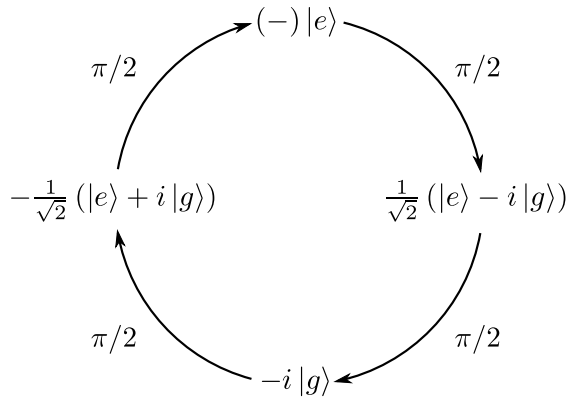


**Fig. 2.1:** Graphic representation of the action of a  $\pi/2$ -pulse on the state of a two level system. The photon number states (e.g. as in  $|e\rangle|n\rangle$ ) are not shown explicitly. The  $(-)$  in front of the excited state indicates the change of the total phase after one full cycle, which is of importance only if there is another state to which it should be compared in measurement.

with the off-resonant Rabi frequency

$$\Omega_n(\Delta) = \sqrt{\Delta^2 + 4\omega_{\text{int}}^2(n+1)}. \quad (2.19)$$

The eigenenergies of the new eigenstates depend on the detuning of the light with respect to the atom transition. This shift in the energy levels is often referred to as the “AC-Stark-shift”. The corresponding eigenstates in the given basis are

$$|n,+\rangle = \cos(\Phi_n/2)|e\rangle|n\rangle + \sin(\Phi_n/2)|g\rangle|n+1\rangle \quad (2.20)$$

$$|n,-\rangle = -\sin(\Phi_n/2)|e\rangle|n\rangle + \cos(\Phi_n/2)|g\rangle|n+1\rangle \quad (2.21)$$

where the angle  $\Phi_n$  is given by

$$\Phi_n = \tan^{-1} \left( \frac{2\omega_{\text{int}}\sqrt{n+1}}{\Delta} \right) \quad (2.22)$$

which converges towards  $\pi/2$  for  $\Delta \rightarrow 0$ . The dressed states are now useful for many applications in the field of quantum optics. Given a prepared state of a two level atom, one can determine the interaction of the atom with (not necessarily resonant) incident light by expressing the initial state in terms of the dressed states. As the dressed states are eigenstates of the total Hamiltonian their time evolution is trivial under application of the time evolution operator. In this way the dynamics can be calculated in the dressed states basis and afterwards (if needed) transformed back to the initial basis.

## 2.4 Far Off Resonance Case

The full Jaynes-Cummings Hamiltonian (2.1) without the rotating wave approximation can also be treated for the far off-resonant case  $\Delta \gg \omega_a$ . Interaction is in this case ruled by the effective Hamiltonian

$$\hat{H}_{\text{eff}} = \hbar\chi [\hat{\sigma}_+ \hat{\sigma}_- + \hat{a}^\dagger \hat{a} \sigma_3], \quad (2.23)$$

where  $\chi$  depends on the photon number  $n$  and the detuning  $\Delta$  [9]. Under this Hamiltonian a state

$$|\Psi(0)\rangle = \frac{1}{\sqrt{2}} (|e\rangle |n\rangle + |g\rangle |n\rangle) \quad (2.24)$$

will evolve according to

$$|\Psi(t)\rangle = \frac{1}{\sqrt{2}} (|e\rangle |n\rangle + e^{-i\chi(\Delta,n)t} |g\rangle |n\rangle), \quad (2.25)$$

a time evolution that Serge Haroche used to non-destructively detect single photons (see Sec. 3.3.3).

### 3 Serge Haroche

One half of the Nobel prize in physics 2012 was awarded to French quantum physicist Serge Haroche. Serge Haroche's main work concentrates on the field of cavity quantum electrodynamics (CQED), i.e. in his case the interaction of Rydberg atoms with single modes in a cavity. In this section we will follow some of the steps of his personal life and scientific career in order to understand how he made his way to the Nobel prize.

#### 3.1 Early Life and Scientific Career

Serge Haroche was born 11 September 1944 in Casablanca, a major city at the Moroccan Atlantic coast, as the son of Albert and Valentine Haroche, both teachers at a local Jewish school. At that time the southern part of Morocco was a French protectorate. However in 1956 Morocco gained independence and Haroche's parents moved to Paris as they felt that they had themselves received and given their children a French education. Regarding his performance in school, Haroche seemed to have no problem settling in, as he was "immediately at the head of [his] class" [10] at his new school in Paris. After his "Baccalauréat"<sup>4</sup> he joined the "école préparatoires" for two years of continuous training and examination to eventually be admitted to one of the French elite universities. Being the best of his year in the national ranking, he was able to join "École Normale Supérieure" (ENS) in 1963 where he studied until 1967 and was taught, among others, by Alfred Kastler<sup>5</sup> and Claude Cohen-Tannoudji.<sup>6</sup> At the end of his studies he was "enthralled by the mysterious beauty of the quantum world" [10] and decided to continue his academic career in the field of quantum physics, more specifically quantum optics. He decided to write a PhD thesis with Cohen-Tannoudji as his supervisor on the dressed states formalism (see Sec. 2.3) and its implications on the description of optically pumped atoms. In the experiments he performed, he used spectral lamps as a light source but it became clear for him that he needed to learn how to apply lasers to his field of research.

After his PhD at ENS, Serge Haroche joined the group of Arthur Schawlow<sup>7</sup> at Stanford University from 1972 to 1973. Shortly before his arrival Theodor Hänsch<sup>8</sup> had joined the group as an associate professor, making him the fourth later Nobel laureate to work with Haroche. Schawlow provided Haroche with a lab room and a pulsed dye laser and told him that "it was up to [him] to find something interesting to do with it" [10]. As Haroche was already familiar with the dressed states formalism and saw the potential of the laser as a much more intense light source compared to classical lamps, he decided to



**Fig. 3.1:** Serge Haroche in 2012.  
Source: nobelprize.org

<sup>4</sup>The French equivalent to the German "Abitur".

<sup>5</sup>Nobel prize for physics in 1966 "for the development of optical methods for studying Hertzian resonances in atoms".

<sup>6</sup>Nobel prize for physics in 1997 "for the development of methods to cool and trap atoms with laser light".

<sup>7</sup>Nobel prize for physics in 1981 "for his contribution to the development of laser spectroscopy".

<sup>8</sup>Nobel prize for physics in 2005 "for his contribution to the development of laser-based precision spectroscopy".

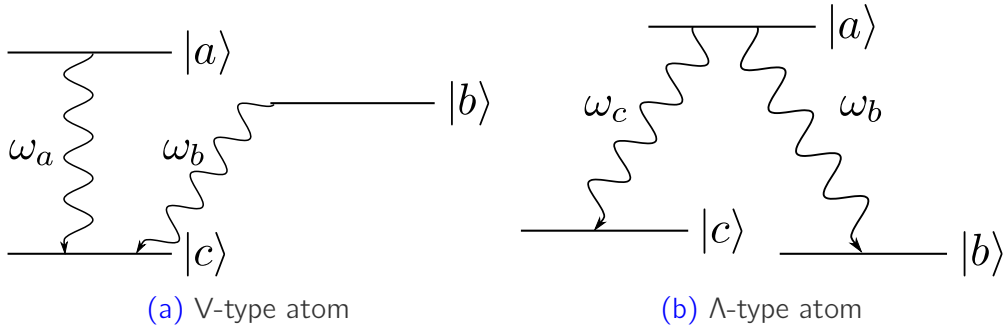


**Fig. 3.2:** Atom level schemes for which there should be quantum beat signals in the emitted intensity in a semi-classical model. In QED only (a) shows quantum beats which is in accordance with experiment.

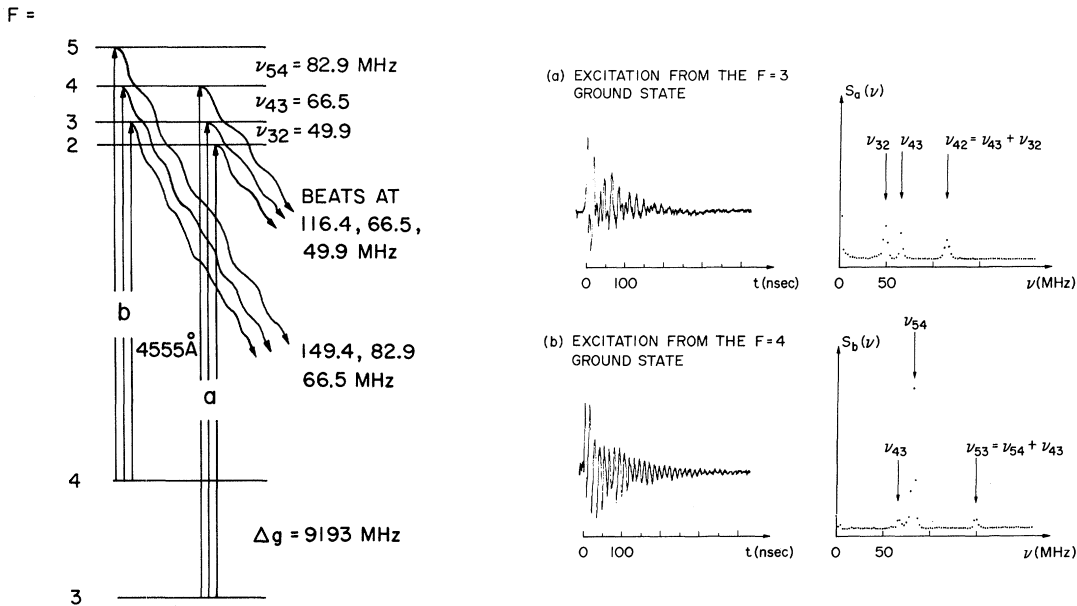
probe quantum beat signals in cesium vapor [11]. The resulting paper will be discussed in Sec. 3.2. Still in Stanford Haroche sent a research proposal on the study of Rydberg atoms to one of the ENS directors and was immediately offered a position and start-up budget. His own research in the labs of ENS started in 1973 and has continued ever since with Rydberg atoms being a central pillar of many experiments.<sup>9</sup> At ENS Haroche had a position as “maître de recherche” that allowed him to fully focus on his research. However he was also keen to teach students, driving him to take on a position as a full professor of physics at Université Paris VI. In the early 1980s Haroche started his research in the field of cavity quantum electrodynamics (CQED) on which all of his later explorations of fundamental quantum mechanical concepts are based. His research on CQED will be addressed with the discussion of some exemplary experiments in Sec. 3.3. At this time Haroche already had a good reputation as a scientist and was offered a position at Harvard in 1981 which he refused. When he was tempted again in 1984, this time by the University of Yale, he accepted and was appointed a professor while at the same time retaining his position in Paris. He kept the chair in Yale until 1993 and during this time was able to run successful experiments on both sides of the Atlantic [12, 15]. In 2001 Haroche was appointed professor of quantum physics at Collège de France [16]. The Collège de France is a prestigious institution at which scientists from different fields give lectures on their current research that are open to the public. In 2009 Haroche was awarded the gold medal of the Centre National de la Recherche Scientifique, one of the highest honors awarded to French scientists once a year.

## 3.2 Quantum Beats

During his postdoc in Stanford Haroche investigated the phenomenon of quantum beats that appear in the fluorescence intensity in some types of atoms when they are excited to a superposition of upper states and decay towards a common lower lying state [11]. Quantum beats were especially interesting as they could only be entirely described by quantum electrodynamics (QED), i.e. in a model in which not only the energy levels of the atom but also the states of the light field are quantized.

The two types of atoms that are interesting with regards to quantum beats are shown in Fig. 3.2. V-type atoms have two upper levels  $|a\rangle$  and  $|b\rangle$  that can decay to a common

<sup>9</sup>See for example [1, 12–14]



- (a) Level scheme of the cesium hyperfine structure. Pulsed excitation from either of the lower levels ( $F=3,4$ ) introduces the two possible sets of quantum beats  $a$  and  $b$  with beat frequencies indicated.

- (b) Recorded intensities (left) and Fourier analysis (right) for the two different types of excitation. The frequency spectrum exhibits characteristic maxima in both cases.

**Fig. 3.3:** Hyperfine structure of cesium and experimentally measured fluorescence intensities, showing a quantum beat signal as predicted by QED.(Source: [11])

lower lying state  $|c\rangle$  but transitions between them are dipole forbidden.  $\Lambda$ -type atoms consist of one upper level  $|a\rangle$  that can decay to two different lower lying levels  $|b\rangle$  and  $|c\rangle$ . Summarizing the QED calculations in [17], for V-type atoms one expects a modulation on top of the intensity signal of the form

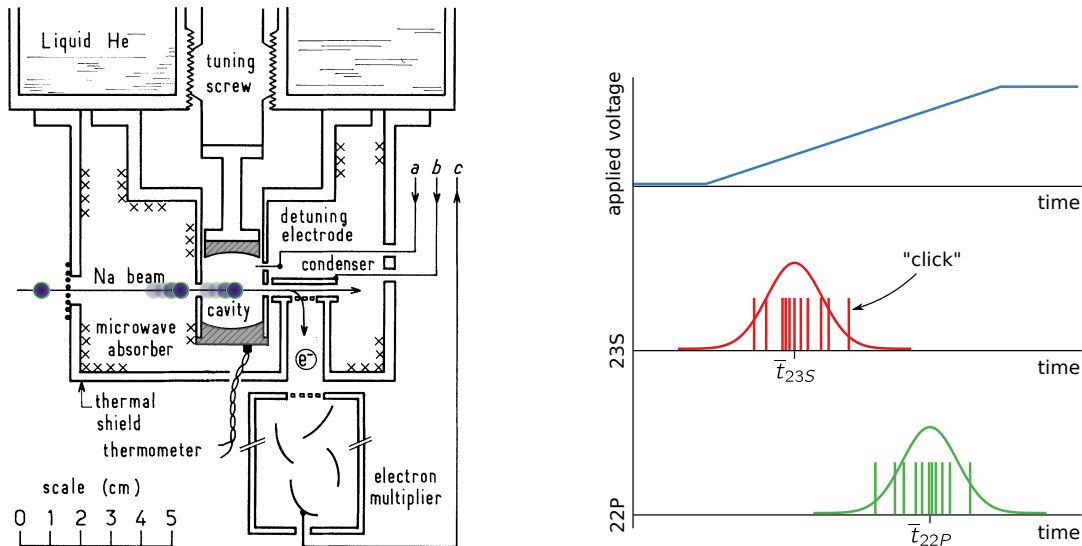
$$I_{tot}(t) = I_0 + I_{beat} \cos \{(\omega_a - \omega_b) t\} \quad (3.1)$$

whereas for  $\Lambda$ -type atoms, the beat term vanishes. This result is in disagreement with a semiclassical approach in which both types show a beat term. However only the QED results are consistent with performed experiments.

The system of interest for Serge Haroche was the cesium hyperfine structure shown in Fig. 3.3a. The frequency bandwidth of the pulsed dye laser is smaller than the splitting of the two lower levels, but large enough to populate all possible upper states. This means that e.g. from the  $F=3$  ground state, the  $F'=2,3,4$  excited states can be populated according to the dipole selection rule. In this way two sets of upper states can be excited, namely  $a$  and  $b$  in Fig 3.3a. The expected beat frequencies are the three difference frequencies between the upper levels.

The experimental results are shown in Fig 3.3b. The fluorescence intensities on the left show a clear oscillating behavior, with an exponentially decaying envelope caused by the characteristic damping of spontaneous emission. The plots on the right show the Fourier spectrum of the intensity signals. In each of them there are three characteristic peaks that correspond to the three beat frequencies indicated in Fig. 3.3a.

The resulting frequencies were in good agreement with other values that had been



- (a) The superconducting cavity in the center can be tuned using a screw and is cooled by liquid helium. After crossing the cavity, the atoms states are detected in the ionization detector.
- (b) The voltage applied to the condenser is increased in time. The different ionization energies of the 23S and the 22P states lead to different electron detection times in the electron multiplier.

**Fig. 3.4:** Experimental setup and ionization detection scheme used to observe cavity enhanced spontaneous emission. (Adapted from [12])

measured for the hyperfine structure of cesium. Although the uncertainties were higher than those of other state of the art spectroscopy methods there was a clear advantage of this method: once one is able to excite the upper states, there is no need to scan for resonance as the full intensity spectrum already exhibits the needed modulation. A very finely tunable laser is thus not necessary. Further, the precision of the method could be improved by increasing the sampling frequency and the total number of sample points taken.

### 3.3 Cavity Quantum Electrodynamics

After his first experiments in quantum optics, Serge Haroche soon turned towards his very own field of research: cavity quantum electrodynamics (CQED). CQED deals with the interaction of light that is confined in a cavity with atoms e.g. passing through it. The cavity can be used to engineer coherent photon number states  $|n\rangle$  with  $n$  going down to 0 or 1. In this regime the quantum nature of light can be revealed. The following section will go through some of the experiments performed by Haroche that revealed or made use of the quantum behavior of photons.

#### 3.3.1 Enhanced Spontaneous Emission

One of the first experiments of the ENS group of Haroche investigated the effect of enhanced spontaneous emission rates of an excited atom flying through a resonant cavity [12]. When an atom prepared in the upper of two levels, separated by  $\hbar\omega = \frac{h\lambda}{c}$ , is brought into a cavity that is tuned to resonance with  $\omega$ , the spontaneous emission rate

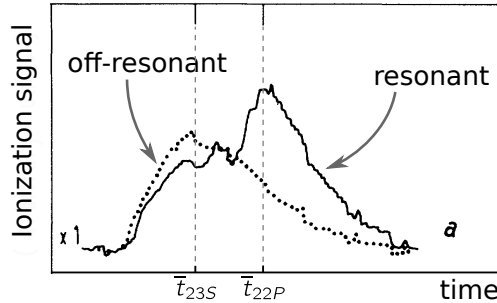


**Fig. 3.5:** Ionization signal of the atoms after crossing the cavity which is either off-resonant (dotted line) or resonant (solid line). An increased population of the 22P state is observed in the resonant case.

will be increased as

$$\Gamma_{\text{cav}} = \Gamma_0 \frac{3Q\lambda^3}{4\pi^2 V} \equiv \Gamma_0 \eta_{\text{cav}}, \quad (3.2)$$

where  $\Gamma_0$  is the natural decay rate,  $Q$  is the Q-value of the cavity and  $V$  its mode volume. Observations of this effect in the optical range (e.g. in Fabry-Perot interferometers) were impossible even for very high Q-values as the volume  $V$  is typically much larger than  $\lambda^3$ . Rydberg atoms played a key role in the detection, as their transitions are typically in the mm wavelength, an order of magnitude in which cavities can be manufactured.

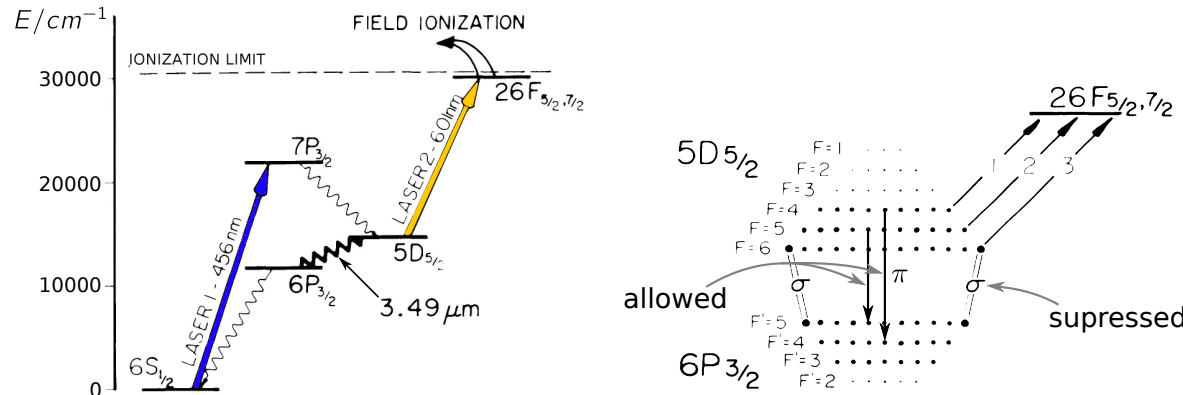
The experimental setup used by Haroche et al. is shown in Fig 3.4a. The central part is the superconducting niobium cavity cooled down to 5.7 K with an estimated Q-value of the order of  $10^6$  and an effective mode volume of  $V = 70 \text{ mm}^3$ , surrounded by an absorbent shielding to isolate it from background radiation. A micrometer screw allows tuning of the cavity's resonance frequency. To detect the increased spontaneous emission rate, sodium atoms are prepared in the 23S Rydberg state. The  $23S \rightarrow 22P$  transition has a wavelength of  $\lambda = 0.88 \text{ mm}$  which makes observation of the effect possible for the given Q-value. The final state of the atoms, after having crossed the cavity, is determined by using a combination of a condenser and a time resolved electron detector. The detection scheme is depicted in Fig. 3.4b, showing the voltage applied to the condenser and two exemplary detection patterns in the electron multiplier as a function of time. One exploits the feature that the 23S state and the 22P state have different ionization energies. Ramping up the voltage with time will thus on average result in different ionization times corresponding to different electron detection times  $\bar{t}_{23S}$  and  $\bar{t}_{22P}$ . When the cavity is tuned to resonance, the share of atoms in the 22P state should increase caused by an increase of the transition rate  $\Gamma_{23S \rightarrow 22P}$ .

This expectation exactly matches the experimental results shown in Fig. 3.5. One sees a clear shift of the peak in the ionization time histogram from  $\bar{t}_{23S}$  to  $\bar{t}_{22P}$  when the cavity is tuned from off-resonance to resonance. That means that tuning the cavity to resonance indeed increases the spontaneous emission rate as predicted by the CQED result (3.2).

Haroche and his group at ENS were the first to give experimental evidence of this CQED effect. But soon others followed. Namely the group of Haroche at Yale who were able to show that also a suppression of certain modes is possible using a similar experiment that will be described in the following section.

### 3.3.2 Suppressed Spontaneous Emission

Another interesting effect that a surrounding cavity can have on the energy states of an atom is the suppression of spontaneous emission. This effect was first experimentally realized by Haroche and his group in Yale in 1986 [15]. When the distance between the



- (a) Level scheme of the used cesium atoms. Before entering the cavity, the atoms are prepared in the  $5D_{5/2}$  state by excitation to  $7P_{3/2}$  and spontaneous emission. The second laser drives the transition  $5D_{5/2} \rightarrow 26F$ .

- (b) Hyperfine structure of the  $5D_{5/2}$  and  $6P_{3/2}$  levels. Due to the polarization dependent cut-off in the cavity, only  $\pi$  transitions are allowed. The  $F=6$  substate of  $5D_{5/2}$  can only decay via  $\sigma$  transitions.

**Fig. 3.6:** Relevant energy levels of cesium and their hyperfine structure. The different colors (blue and yellow) correspond to the two different lasers that are used. (Source: [15])

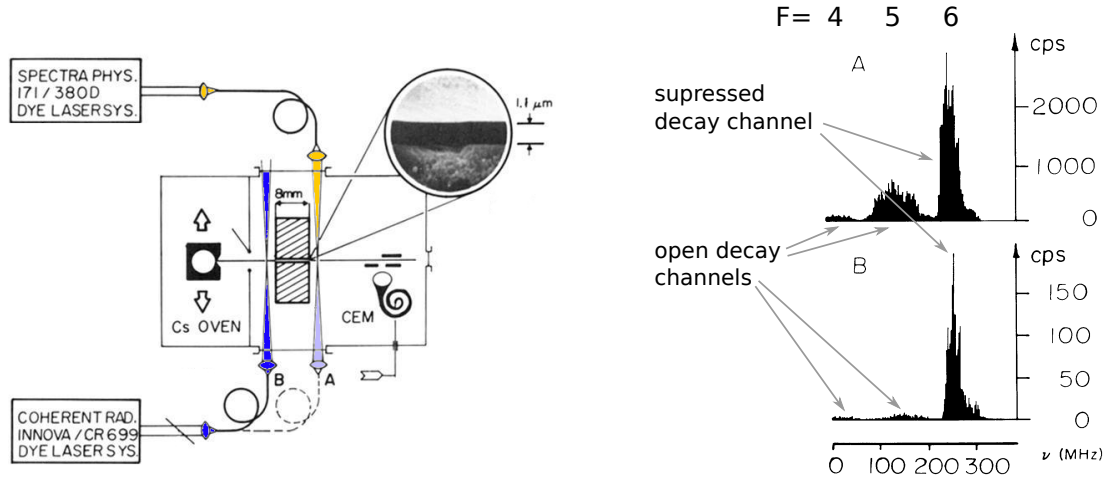
mirrors of the cavity  $d$  becomes smaller than half the wavelength  $\lambda$  of a certain transition in the atom, i.e.

$$d < \frac{\lambda}{2}, \quad (3.3)$$

all transitions of this wavelength that are polarized parallel to the mirror surface are suppressed. A pictorial explanation would be the following: as the spontaneous emission rates depend on the vacuum fluctuations, but the boundary conditions imposed by the mirrors do not allow modes that fulfill (3.3), spontaneous emission for these modes is inhibited. Nonetheless, any transition polarized perpendicular to the mirrors is still allowed and can even be enhanced. When a magnetic field is applied perpendicular to the mirror surfaces, the first type of radiation is  $\sigma$  polarized while the latter is of  $\pi$  polarization. So to observe the anomalous survival of a state caused by a cavity, one needs to identify a state from which only  $\sigma$  decay is possible.<sup>10</sup>

Haroche and his group chose to use cesium atoms and identified the  $5D_{5/2}$  level to be suited for their purpose. As can be seen in the level scheme in Fig. 3.6a, the  $5D_{5/2}$  level decays to the  $6P_{3/2}$  level via emission of  $3.49 \mu\text{m}$  radiation. Looking at the hyperfine structure of this transition shown in Fig. 3.6b we see that the  $F=6$  substate of  $5D_{5/2}$  can only decay via  $\sigma$  emission.

<sup>10</sup>In principle one could also calculate the change in the decay rate of a state depending on the share of  $\pi$  and  $\sigma$  transitions, but the survival of an else decaying state is easier to measure.



- (a) The cavity used to cut off certain modes is  $1\text{ }\mu\text{m}$ . Two lasers are used in cw mode, colored corresponding to the transitions shown in Fig. 3.6a. A condenser with constant voltage together with a channel electron multiplier (CEM) is used to detect the 26F state similar to the previous experiment.
- (b) Resulting counting rates in the CEM as a function of the frequency of the detection laser (yellow). Shown for atoms not having crossed (A) and having crossed (B) the cavity. Only atoms in the F=6 substate survive the flight through the cavity.

**Fig. 3.7:** Setup and experimental results showing the suppression of spontaneous emission of some of the transitions in the cesium hyperfine structure. (Adapted from [15])

The setup that exploits these features of cesium is shown in Fig. 3.7a. A directed beam of cesium atoms is leaving an oven. First a pumping laser (blue) is used to prepare the atoms in the  $5D_{5/2}$  state (see Fig. 3.6a). Next the atoms pass through the  $1.1\text{ }\mu\text{m}$  wide cavity, made of gold coated fused silica blocks. A cavity of this size will suppress any of the  $5D_{5/2} \rightarrow 6P_{3/2}$   $\sigma$ -transitions and thus suppress any transition of the F=6 substate of  $5D_{5/2}$  (see Fig. 3.6b). A  $240\text{ }\mu\text{T}$  magnetic field perpendicular to the mirror surfaces will align the atoms along a common axis. After the cavity the atoms fly through the beam of the detection laser (yellow) that can be tuned around the  $5D_{5/2} \rightarrow 26F$  transition hence selectively pumping atoms from the hyperfine levels of  $5D_{5/2}$  to the Rydberg state 26F. Any atom in the 26F state will then be ionized in a condenser with a constant voltage of 1 kV, the ionization electron being detected in a channel electron multiplier.

In this way (again using the properties of Rydberg atoms) the relative populations of the several substates of  $5D_{5/2}$  can be determined. The resulting counting rates of the CEM are shown in Fig. 3.7b. The upper histogram shows the counting rates depending on the resonant substate with the pumping laser placed directly in front of the detection laser. This corresponds to the relative populations resulting from the pumping process. The lower histogram shows the counting rates for the case in which the atoms interact with the pumping laser before entering the cavity and are pumped to the 26F state by the detection laser after having traversed the cavity. Besides the fact that the counting rates are generally lower, due to a loss of atoms in the cavity, one sees that the peaks for the F=4 and F=5 substates of  $5D_{5/2}$  almost vanish completely compared to the peak of the F=6 substate. This is experimental evidence that the decay of F=6 is strongly suppressed by the surrounding cavity.

The preceding experiments all show the quantum behavior of light, yet the wave function of the photon was not observed in a direct manner. This would change with Haroche's experiments on quantum non demolition measurement of photons, which will be introduced in the next section.

### 3.3.3 Quantum Non Demolition Measurement of Photons

Many experiments (like the ones in the preceding sections) show traces of the quantum nature of photons. However "in-vito", i.e. non destructive, measurement of the photons wavefunction was not performed until 2007,<sup>11</sup> when Haroche and his group at ENS introduced the first working experimental setup able to count an individual photon without destroying it. To implement the quantum non demolition (QND) measurement of photons, Haroche used many of the things he had learned about Rydberg atoms and their interaction with light in a cavity. A proof of concept paper about the technique had already been published in 1999 [14], but it took Haroche and his group another seven years to create a cavity with a Q-value so high that it could store photons with a typical lifetime of  $\tau_\gamma = 0.1$  s [18]. In this cavity thermal photons would survive long enough to interact with several hundreds of single atoms passing through the cavity [1].

An artists view of the setup is shown in Fig. 3.8a. Of course in reality the whole setup is vacuumized, shielded from the environment and cooled down to a few K similar to the setup shown in Fig. 3.4a. The cavity itself is cooled down to 0.8 K, a temperature at which the possibility of two thermal photons being excited is only 0.3%. The lifetime of resonant photons in the cavity was estimated to be 0.129(3) s by exciting a classical microwave in the cavity and measuring its ring-down time. A beam of single rubidium atoms is flying through the setup from left to right. In  $B$  they are pumped to a highly excited Rydberg state  $|e\rangle \equiv |51\rangle$ .  $R_1$  and  $R_2$  both apply  $\pi/2$ -pulses to the atom, tuned to resonance with the  $|e\rangle \rightarrow |g\rangle \equiv |50\rangle$  transition. This setup is also called "Ramsey interferometer". The central part is the superconducting cavity, which is off resonant to the atoms and can or cannot contain a thermal photon (the possibility of two thermal photons will be neglected). The atoms will obtain a phase shift due to the photon field in the cavity, that depends on the number of photons. At  $D$  the atoms will be detected either in the ground or in the excited state, following the principle of ionization detection introduced in Sec. 3.3.1.

To understand how exactly this setup measures the number of photons in the cavity (as long as it is 0 or 1) we will follow the wave function of the atom in a step by step manner. Initially the atoms are in the ground state and are excited to a Rydberg state in  $B$  giving

$$|\Psi_B\rangle = |e\rangle.$$

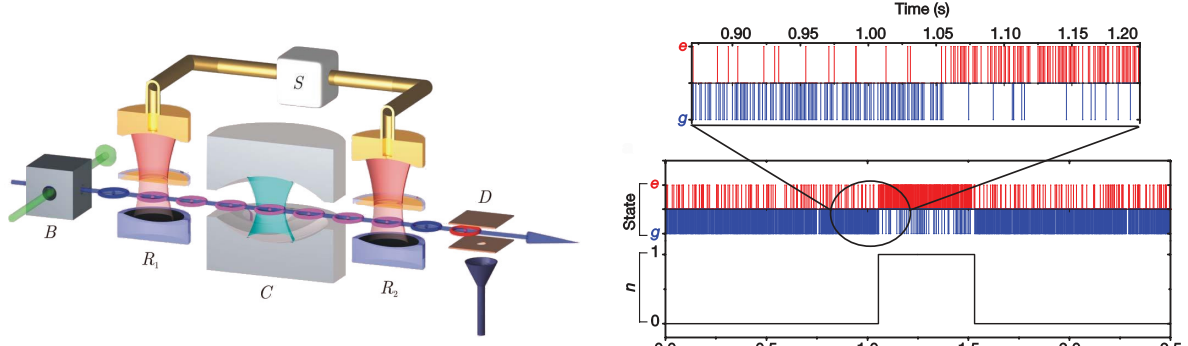
Next in  $R_1$  a  $\pi/2$ -pulse will be applied to the atoms. According to Fig. 2.1 this will take the wave function to a superposition of excited and ground state

$$|\Psi_{R_1}\rangle = \frac{1}{\sqrt{2}} (|e\rangle - i|g\rangle).$$

As the cavity is tuned to be far off resonance with the atoms, the time evolution of the wave function in the cavity will follow (2.25), introducing a phase shift in the superposition

---

<sup>11</sup>For example a photodiode detects photons by absorption of the photon and creation of an electron-hole pair, that means the photons are destroyed in the detection process.



(a) Artist view of the setup used for QND measurement of photons.  $B$  prepares the atoms in a Rydberg state,  $R_1$  and  $R_2$  both apply a  $\pi/2$ -pulse to the atoms,  $D$  uses ionization detection similar to Fig. 3.4b,  $C$  is the superconducting cavity, cooled down to 0.8 K and detuned from the atom transition.

(b) Experimental results of the thermal photon detection. The upper trace shows whether the atom was detected in excited (red) or ground (blue) state. The lower trace shows the result of a majority vote, decreasing statistical error and fluctuations. A single photon was first detected at  $t_0 \approx 1.05$  s and observed by several hundreds of atoms during  $\tau \approx 0.5$  s.

**Fig. 3.8:** Experimental setup and results of the first realization of quantum non demolition measurement of photons. (Source: [19])

state of the atoms after the cavity

$$|\Psi_{\text{cav}}\rangle = \frac{1}{\sqrt{2}} (|e\rangle - ie^{-i\Phi(\Delta, n)} |g\rangle).$$

To calculate the exact phase shift, one has to take into account the detuning of the cavity, the resonant Rabi frequency, the number of photons in the cavity, the transverse profile of the cavity mode and the time of flight of the atoms. But the key point is that some of these parameters, namely the detuning and the time of flight, can be adjusted such that

$$\Phi(\Delta, n) = \begin{cases} 0 & \text{for } n = 0 \\ \pi & \text{for } n = 1 \end{cases}$$

which results in the wave function

$$|\Psi_{\text{cav}}\rangle = \begin{cases} \frac{1}{\sqrt{2}} (|e\rangle - i|g\rangle) & \text{for } n = 0 \\ \frac{1}{\sqrt{2}} (|e\rangle + i|g\rangle) & \text{for } n = 1 \end{cases}$$

At  $R_2$  the atoms will receive another  $\pi/2$ -pulse which, again following Fig. 2.1, will transform the wave function to

$$|\Psi_{R_2}\rangle = \begin{cases} i|g\rangle & \text{for } n = 0 \\ -|e\rangle & \text{for } n = 1 \end{cases}$$

So by detecting in which Rydberg state the atoms are at  $D$ , one obtains information if there are 0 or 1 photons in the cavity. Note that the global phase of the wave function does not play a role in any physical measurement. The photon however was not absorbed

by the atom, due to the far off detuning of the cavity and can be detected by the following atom as well until it changes its state again caused by external perturbation.

One resulting observed pattern is shown in Fig. 3.8b. Fluctuations that appear due to statistical uncertainties of the detection scheme are taken care of by plotting the majority vote, that means the classification of each event  $n$  is based on the results of  $n$  and the seven preceding events. The shown trace thus shows a photon appearing due to fluctuations between thermal states and surviving in the cavity for approximately half a second, corresponding to a traveled distance of light of around 150 000 km folded in the cavity.

Haroche and his group found many other applications of this or similar setups, like engineering multi particle entanglement [4] and Schrödinger cat states [2] or observing the time evolution of photon number states in a cavity [20]. One could in principle dive arbitrarily deep into the principles of quantum optics just with the experiments of Serge Haroche at hand, but this would go far beyond the scope of this term paper<sup>12</sup>. Summarizing his work from a current perspective, it shows an impressive continuity and coherence and definitely deserves<sup>13</sup> a Nobel prize as it tackled numerous fundamental topics of quantum mechanics and quantum electrodynamics.

---

<sup>12</sup>...and the time available to the author.

<sup>13</sup>The author is aware of the fact that this judgement is not up to him, but anyways...

## 4 David Wineland

The second half of the Nobel prize in physics 2012 was awarded to the American quantum physicist David Wineland. David Wineland's work was driven by the will to capture and take full control of single ions, leading for example to the development of Doppler cooling. In this section we will first address his early life and scientific career and then introduce important experimental methods he established.

### 4.1 Early Life and Scientific Career

David Wineland was born the same year as Serge Haroche on February 24, 1944, in Wauwatosa, Wisconsin. His family moved to Sacramento, California in 1947 where he grew up and went to college. He describes his parents as marked by the great depression emphasizing "the importance of frugality and getting a good education" [21]. Having finished high school in 1961, Wineland enrolled for a Math Major at the University of California. He soon realized that, working hard enough, he could make it to the top of his class. Still in his junior year he changed his university and subject and took up a Physics Major at Berkeley. At the end of his undergraduate studies in physics he was not sure where to apply for a Master and PhD, but asking his classical mechanics teacher helped a lot: "he recommended Harvard, so I applied there". This said he started his studies at Harvard University in 1965 and soon joined the group of Norman Ramsey.<sup>14</sup> There he got first in contact with experimental physics and decided to write his PhD thesis about the hyperfine structure of deuterium [22]. In Ramsey's group, a working hydrogen maser had recently been accomplished and his goal was to realize similar setups for all isotopes of hydrogen. After his PhD ended in 1970, Wineland joined the group of Hans Dehmelt<sup>15</sup> who was at that time working on the measurement of the anomalous magnetic moment of the electron. It became clear that the most exact measurements would be performed on single trapped electrons, so Wineland's goal was to trap a cloud of electrons and boil them out one by one until only a single one would be left [23]. During that time he became hooked up on precision measurement and, having already learned a lot about the trapping of charged particles, wanted to explore the field of ion spectroscopy.

Looking for academic positions after his time as a postdoc he found one that fully met his demands. The National Bureau of Standards (NBS, later National Institute for Standards and Technology) was looking for somebody to join the time and frequency domain and set up and calibrate a working cesium clock as a new time standard. Within one year and a half, Wineland and his colleagues had calibrated the clock to produce the new standard second. At that time there were plans for the NBS to become more involved in basic research and consequently, in 1977, Wineland got lab space and was joined by his first group members to work on trapping and spectroscopy of ions. Up to today, he is the

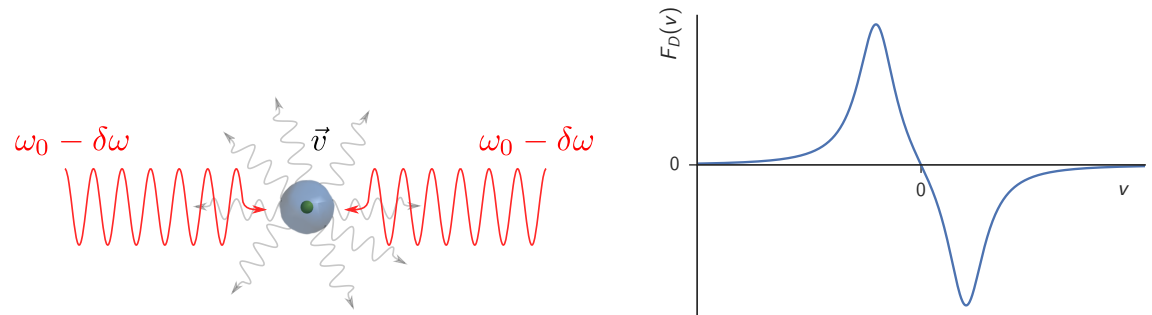


**Fig. 4.1:** David Wineland in 2012.

Source: nobelprize.org

<sup>14</sup>Nobel prize in physics 1989 "for the invention of the separated oscillatory fields method and its use in the hydrogen maser"

<sup>15</sup>Nobel prize in physics 1989 "for the development of the ion trap technique".



- (a) The principle setup of Doppler cooling: two laser beams, red-detuned to a transition frequency of the atom  $\omega_0$  shine in on the atom from opposite directions.
- (b) Force profile as a function of the velocity acting on an atom in a two-beam Doppler cooling configuration.

**Fig. 4.2:** Principle of Doppler cooling and the resulting velocity dependent force profile.

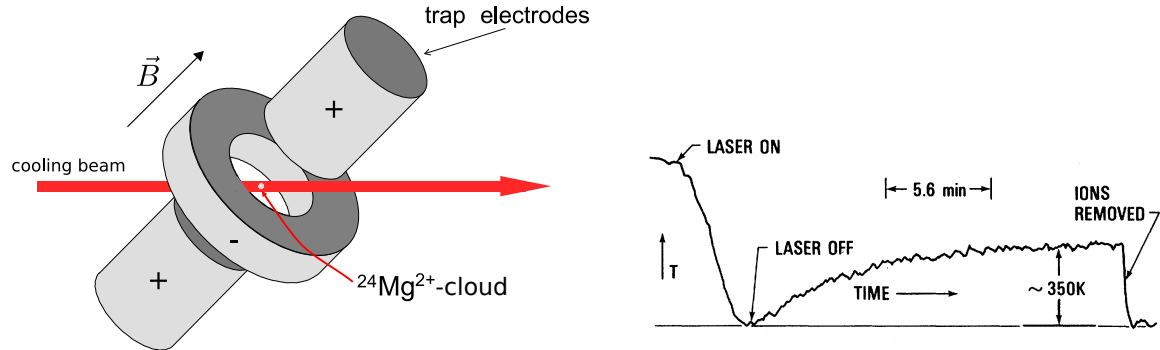
group leader of the ion storage group at NIST with three of the four founding members still on board. Their first goal was to demonstrate the effect of laser cooling on trapped ions, an idea that had been proposed together by Dehmelt and Wineland in 1975 [24]. They were under quite some pressure as Wineland had heard from Dehmelt that he had taken a sabbatical and joined the group of Peter Toschek in Heidelberg with the same aim. Within only one year they had the first results and handed them in for publication only one day apart from Dehmelt and Toschek [25, 26].<sup>16</sup> Their experiment will be discussed in Sec. 4.2. From that day on, Wineland and his group continued to push the limits of single ion control for example by trapping single ions in 1981 [27], demonstrating ion quantum jumps in 1986 [28], inventing the mechanism of resolved sideband cooling in 1989 [29] or implementing the first quantum logic gate in 1995 [30]. Similar to the group of Serge Haroche they found many applications of their methods to the fundamental issues of quantum mechanics like many particle entanglement [5] or observation of the time evolution of pure quantum mechanical states [31].

In the following sections we will explore some of the methods and applications developed by Wineland et al. in their chronic order.

## 4.2 Doppler Cooling

The idea that atoms could be slowed down using a red-detuned laser was first simultaneously proposed by Hans Dehmelt and David Wineland [24] and Theodor Hänsch and Arthur Schawlow [32] in 1975. Wineland and his group were the first to publish experimental results that showed the desired effect [25] in 1978. The idea of Doppler cooling, illustrated in Fig. 4.2a, is the following: in a 1D setup one shines two laser beams onto an atom from opposite directions. Both laser beams are red-detuned by  $\delta\omega$  with respect to a transition of the atom  $\omega_0$ . If the atom now moves towards one of the beams, let's say with velocity  $+v$ , it will be shifted to resonance by the Doppler effect (thus the term Doppler cooling) and absorb more photons from this direction, taking from each the momentum

<sup>16</sup>However Dehmelt and Toschek beat them by one day.



(a) Setup used to Doppler cool a cloud of magnesium ions. The ions are confined in a Penning trap with a red detuned laser beam going through the center of the trap.

(b) Ion temperature as a function of time. The ions were heated up before a cooling laser was switched on. After switching off the laser, the ions are allowed to rethermalize.

**Fig. 4.3:** Setup used to cool down a cloud of magnesium ions and the resulting temperature evolution. (Sources: [25, 34])

$-\frac{\hbar\omega_0}{c}$ . As the atom reemits the photons isotropically, it will feel an overall force opposite to its direction of movement. The force as a function of the velocity is given by

$$F_D(v) = \frac{\hbar\omega_0 I_{rel}}{2c\tau} \left[ \frac{1}{1 + (2\tau(\delta - v\omega_0/c))^2} - \frac{1}{1 + (2\tau(\delta + v\omega_0/c))^2} \right] \quad (4.1)$$

where  $\tau$  is the lifetime of the state and  $I_{rel}$  the light intensity relative to the saturation intensity [33]. The resulting force profile is shown in Fig 4.2b. We see that as long as the atom moves around a velocity of  $v = 0$ , it will experience a slow down force. We note however that the Doppler force does not confine the atoms to a certain position. For this one has to expand a setup by other features.

The setup that was used by Wineland et al. to demonstrate Doppler cooling is shown in Fig 4.3a. A cloud of  $^{24}\text{Mg}^{2+}$  ions is confined in a Penning trap, made of two positive end caps, a negative ring electrode and a magnetic field along the axis of the end caps. A notable difference to the simplified scheme shown in Fig 4.2a is that there is only a single red-detuned laser beam passing through the center of the trap. This is because the atoms are confined in a harmonic trap. The laser beam is aligned with the axis of the harmonic movement of the atoms in the trap, so any time the atoms move towards the beam, they will be slowed down. In contrary to the free case, a second laser is hence not necessary. The results of the experiment are shown in Fig. 4.3b. The signal that was recorded is the current in the trap electrodes induced by the movement of the charged particles in the trap and therefore proportional to  $NT$  with  $N$  being the number of particles in the trap and  $T$  their temperature. A significant particle loss during the time of the experiment could be ruled out, and thus the signal is directly proportional to the particles' temperature. The atoms were first heated up by the cooling laser detuned to *higher* frequencies and then cooled down by the same laser detuned to lower frequencies until they reached a minimum value around 40 K. The cooling laser was then switched off completely to allow the atoms to rethermalize with their environment. The temperature curve clearly shows the effectiveness of the laser cooling principle.

Cooling down clouds of ions was already a step towards measuring atomic spectra more exactly as it would reduce the effects of Doppler broadening. The idea to continue towards

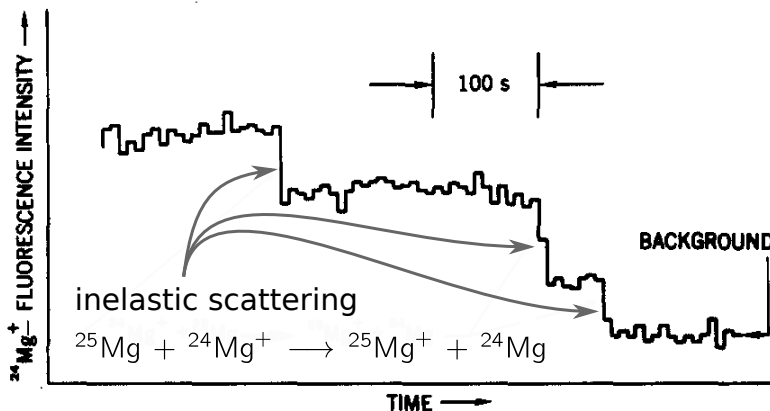
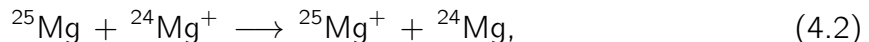


**Fig. 4.4:** Fluorescence intensity over time, as the ions are driven out of the trap by the indicated inelastic scattering process. The final step corresponds to only a single ion being left in the trap. (Adapted from [27])

even higher precision was to isolate single ions as Wineland had already done with electrons during his postdoc in the group of Hans Dehmelt.

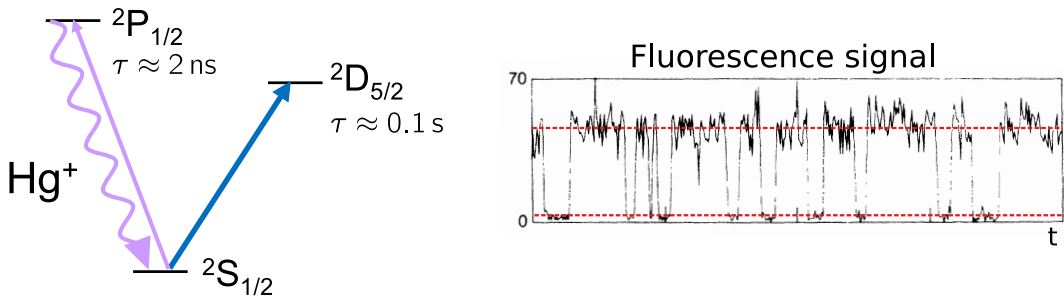
### 4.3 Trapping Single Ions

The typical procedure to trap single particles is to first trap an ensemble of particles and then apply a process by which the particles are kicked out of the trap one by one until there is only a single one left. Wineland and his group were first able to isolate single ions in a Penning trap in 1980, using  $^{24}\text{Mg}^+$ -ions. The experimental setup is similar to the one which demonstrated laser cooling shown in Fig. 4.3a. The laser beam is now additionally aligned slightly off the trap center against the cyclotron movement of the ions to cool down radial degrees of freedom as well. In order to reduce the number of ions in the trap, a beam of  $^{25}\text{Mg}$  atoms was pointed towards the  $^{24}\text{Mg}$  ions in the trap. Eventually the atoms and ions would undergo an inelastic scattering process of the type



exchanging one electron. The  $^{25}\text{Mg}$  ions, having a different cyclotron frequency due to their higher mass, could then be selectively driven out of the trap by radio frequency excitation and the  $^{24}\text{Mg}$  atoms, being neutral, are no longer confined in the trap. The number of atoms is surveyed by measuring the intensity of the emitted fluorescence light, which is again proportional to the number of trapped ions. A resulting intensity vs time curve is shown in Fig. 4.4. The last step in the fluorescence intensity, around 50 s long, coincide with a single trapped ion.

The ability to trap single ions permitted many experiments that had until then been impossible. All of the following experiments were only feasible with single ions, as any interaction with other trapped ions would greatly perturb the evolution of the ions' wavefunction.



- (a) Level scheme of  $\text{Hg}^+$  used in the quantum jumps experiment. The  $\text{S} \rightarrow \text{P}$  transition is used for cooling and detection. The weaker  $\text{S} \rightarrow \text{D}$  is the “quantum jump” transition.
- (b) Fluorescence signal when both transitions are laser driven. The upper fluorescence level corresponds to the ion in the ground state, the lower one to the ion excited to the  $2\text{D}_{5/2}$  state.

**Fig. 4.5:**  $\text{Hg}^+$  level scheme and resulting fluorescence signal exhibiting jumps in the  $2\text{S}_{1/2} \rightarrow 2\text{D}_{5/2}$  transition. (Adapted from [34] and [28])

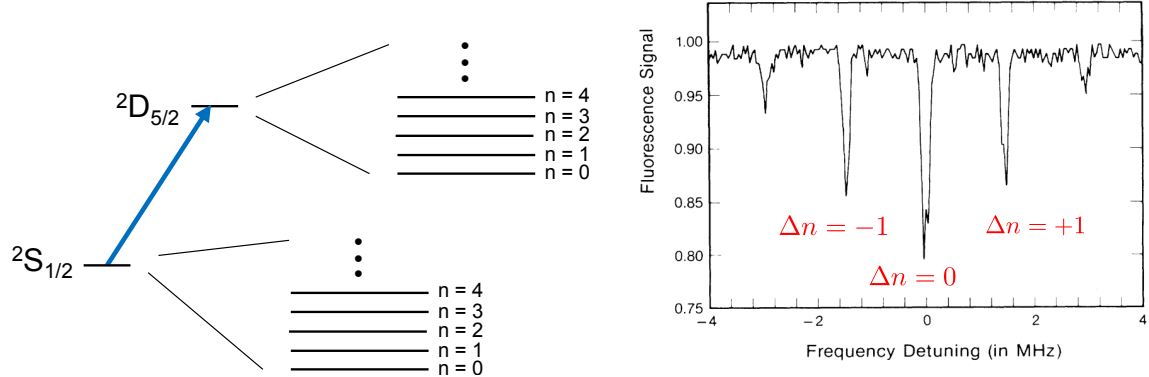
## 4.4 Ion Quantum Jumps

Quantum jumps, the non-continuous transition of a quantum between its energy states, are one of the most fundamental assumptions of quantum mechanics. Nonetheless they have not been observed directly until the mid 1980s. Their observation in ions necessitates a single ions as any ensemble effects would smooth out the discreteness of appearing quantum jumps. David Wineland’s group was among the first to demonstrate quantum jumps in the internal energy state of a single trapped ion in 1986 [28].

The principle of quantum jump detection needs two transitions on different timescales, like shown for the mercury ion in Fig. 4.5a. One transition, in this case  $2\text{S}_{1/2} \rightarrow 2\text{P}_{1/2}$  with  $\lambda_{S \rightarrow P} = 194 \text{ nm}$ , is driven by a laser to cool down the atom and record its fluorescence intensity. As long as the ion is in the ground state, it will be constantly pumped to the  $2\text{P}_{1/2}$  state and reemit a photon with an average rate of  $0.5 \text{ ns}^{-1}$ . Additionally a second much weaker transition, in this case the dipole forbidden  $2\text{S}_{1/2} \rightarrow 2\text{D}_{5/2}$  with  $\lambda_{S \rightarrow D} = 281 \text{ nm}$ , is driven by another laser. If the ion absorbs one of the  $\lambda_{S \rightarrow D}$  photons and “jumps” to the  $2\text{D}_{5/2}$  state, the fluorescence on the first transition will suddenly stop, resulting in a discrete step in the recorded fluorescence signal. As the lifetime of the weak transition is much longer, one can in this way probe the state of the atom with the rate of  $0.5 \text{ ns}^{-1}$ .<sup>17</sup> A resulting trace of the fluorescence signal is shown in Fig. 4.5b, showing sudden steps in the intensity that correspond to jumps on the  $2\text{S}_{1/2} \rightarrow 2\text{D}_{5/2}$  transition. This pattern is similar to the one observed by Serge Haroche in the case of photons (Fig. 3.8b) with the difference that the weak transition is still much more frequent than the appearance of a single photon.

In the same year also the group of Hans Dehmelt at Washington University and the group of Peter Toschek in Heidelberg were able to show quantum jumps of a trapped ion [35, 36]. Since then, quantum jumps have also been observed for other systems like photons, electrons or even molecules [1, 37, 38].

<sup>17</sup>In experiment the probing rate is of course limited by the integration time of the intensity measurement.



(a) Closeup of the level scheme of the trapped  $\text{Hg}^+$  ion, including the motional splitting of the  $^2\text{S}_{1/2}$  and the  $^2\text{D}_{5/2}$  state in the trap.

(b) Intensity as a function of detuning of the S→D laser. The discrete minima, reoccurring at fixed frequency intervals correspond to resonance between different motional levels.

**Fig. 4.6:** Scheme of quantized motional states of an ion in a trap and the resulting intensity signal. Again the fluorescence intensity of the “probing” transition S→P was used to detect whether the ion is in the ground or the metastable D state. (Adapted from [39] and [34])

## 4.5 Sideband Cooling

Single ions could be Doppler cooled down to low temperatures, but the lowest motional state in the trapping potential was still out of reach. This was about to change with the resolution of motional sideband in trapped ions [39] in 1987 and the mechanism of resolved sideband cooling in 1989 [29]. Wineland and his group realized that, making use of the recoilless absorption of ions in a trap similar to the Mössbauer effect and finely tunable lasers, they were able to cool down single ions to their absolute motional ground state in an ion trap. As in the quantum jump experiment they made use of the two transitions in the  $\text{Hg}^+$  ion depicted in Fig. 4.5a, but this time the fluorescence signal was recorded as the laser driving the  $S \rightarrow D$  was detuned by a few MHz around resonance. The resulting trace in Fig. 4.6b shows intensity minima at a detuning of multiples of a frequency  $\omega_{\text{trap}}$  around resonance. That means that at these frequencies the ion is more likely to undergo the  $S \rightarrow D$  transition. This behavior can be explained by considering that the motional energy of an ion in a harmonic trapping potential will be quantized, resulting in energy levels separated by  $\hbar\omega_{\text{trap}}$  where  $\omega_{\text{trap}}$  is a characteristic angular frequency. For  $\omega_{\text{trap}}$  much smaller than the internal resonance frequency  $\omega_{S \rightarrow D}$  this will result in an energy level in which any internal states will show sublevels corresponding to the motional quantum  $n$  like shown in Fig. 4.6a.<sup>18</sup>

How can a laser that resolves the motional levels of the trapped atom now be used to cool the atom to its motional ground state? To explain this one first needs to introduce the Lamb-Dicke regime, characterized by

$$\eta^2(2n+1) \ll 1, \quad (4.3)$$

where  $\eta$  is the Lamb-Dicke parameter and  $n$  the motional quantum number. Further  $\eta$  is

<sup>18</sup>This is in principle equivalent to the dressed states that appear in the treatment of the Jaynes-Cummings Hamiltonian (see Sec. 2.3) if we substitute the motional quantum  $n$  by the photon number  $N$ .

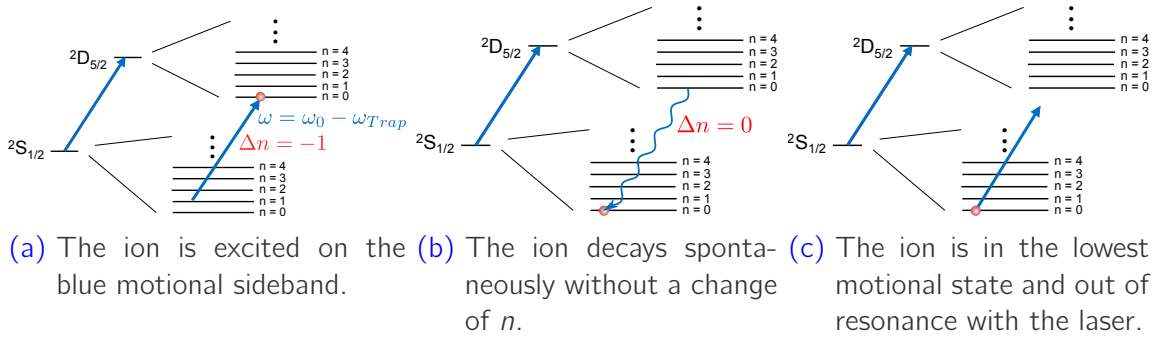


**Fig. 4.7:** One cycle of resolved sideband cooling, pumping the ion from  $n = 1$  to the lowest motional state  $n = 0$ .

given by

$$\eta^2 = \frac{\omega_R}{\omega_0}, \quad (4.4)$$

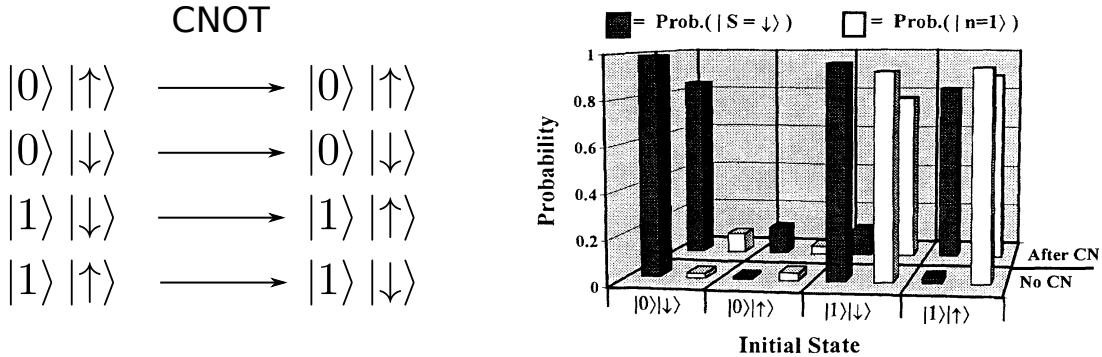
where  $\omega_0$  is the frequency of the laser, in our case driving the S $\rightarrow$ D transition, and  $\omega_R$  corresponds to the recoil energy  $E_R = \hbar\omega_R = \frac{\hbar^2\omega_0^2}{2mc^2}$  that an atom gains upon absorbing a photon of energy  $\omega_0$ . When  $\eta^2$  and  $n$  are both small, i.e. when (4.3) is fulfilled, the process of spontaneous emission takes place on a different energy scale than the change of the motional state. This means that in the Lamb-Dicke regime, the motional quantum  $n$  of a trapped ion will most likely not change upon spontaneous emission of a photon. The described mechanisms can now be combined to the so called resolved sideband cooling. The process is schematically shown in Fig. 4.7. Assume the following setting: an ion is sitting in its internal ground state and the motional state  $n$  for which the Lamb-Dicke condition (4.3) is fulfilled. A laser is shone in on the red motional sideband frequency  $\omega_0 - \omega_{\text{trap}}$ . The dynamics can then be described in three steps:

- The ion absorbs one photon from the laser and will undergo the transmission from  $|g\rangle|n\rangle$  to the excited state  $|e\rangle|n-1\rangle$  due to the red sideband condition.
- From the excited state  $|e\rangle|n-1\rangle$  the ion will decay spontaneously to  $|g\rangle|n-1\rangle$  without changing its motional state due to the Lamb-Dicke regime.
- The preceding two steps repeat until the ion is in the motional ground state of the trap  $|g\rangle|0\rangle$  which is a dark state as there is no state  $|e\rangle|-1\rangle$  fulfilling the resonance criterion.

This procedure was first demonstrated to work by Wineland and his group in 1989 [29]. Cooling the ion to the motional ground state not only increased the precision of frequency measurement, but was also the foundation for later experiments in which full control of the motional and internal states was needed. A good example for this is the implementation of a quantum controlled-NOT gate, which will be discussed in the next section.

## 4.6 Quantum Logic Gate

Quantum computing has become a thriving field of theoretical physics, experimental physics and computer sciences with even companies joining the search for efficient and



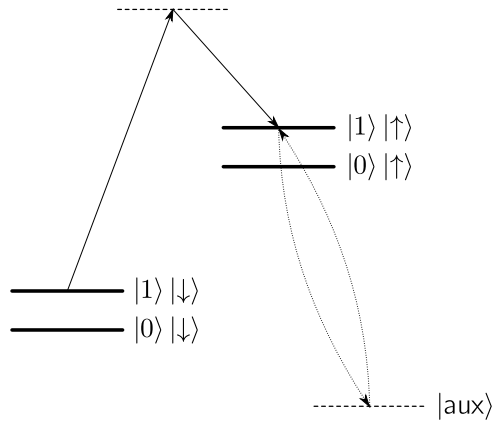
- (a) Theoretical action of a CNOT gate on the four possible pure states of a two qubit system. The first qubit acts as the control qubit, the second as the target qubit.
- (b) Truth table of the experimentally realized CNOT gate. The white bars correspond to the motional qubit (control qubit), the black bars correspond to the internal qubit (target qubit).

Fig. 4.8: Theoretical (a) and experimental (b) truth table of a quantum CNOT operation. (Adapted from [30])

high fidelity implementations, since it was first proposed in the 1980s by Feynman and others [40]. The fundamental difference to classical computing is that information is no longer stored in classical bits that can be either 0 or 1 but in quantum bits (qubits)  $|0\rangle$  and  $|1\rangle$  that can occur in any superposition according to the principles of quantum mechanics. This introduces new possibilities of coding, e.g. Peter Shor proposed a qubit based algorithm to factorize integers in polynomial time in 1994 [41].<sup>19</sup> The implementation of quantum algorithms requires the experimental realization of qubits and of quantum logic gates, i.e. processes that perform basic logic operations on qubits without destroying their quantum nature. In 1995 Wineland and his group realized that both would be possible with cooled down, trapped single ions and demonstrated the first working quantum logic gate, namely a controlled-NOT gate [30].

A controlled-NOT (CNOT) gate has two qubits of input: the control qubit and the target qubit. Whenever the control qubit is  $|1\rangle$ , the target qubit is flipped, when the control qubit is  $|0\rangle$ , the qubits remain unchanged. The resulting operation on the four possible pure states of a system consisting of two qubits is shown in Fig. 4.8a. As Wineland's group was already able to control the motional and the internal state of trapped ions, the idea was to use each of them to store one qubit of information. Confining the ion to the lowest two motional states, the control qubit would then be  $|n\rangle$  with  $n = 0, 1$ . As long as any operation is shorter than the lifetime of the internal state, the internal state being  $|\uparrow\rangle$  or  $|\downarrow\rangle$  corresponding to the ion in the excited or ground state, can be used as the target qubit. Experimentally these states were the motional states of a trapped  $\text{Ba}^+$  ion and its hyperfine states  $|\uparrow\rangle = {}^2\text{S}_{1/2} |F = 2, m_F = 2\rangle$  and  $|\downarrow\rangle = {}^2\text{S}_{1/2} |F = 1, m_F = 1\rangle$ . To implement the CNOT operation a third auxiliary state  $|\text{aux}\rangle = {}^2\text{S}_{1/2} |F = 2, m_F = 0\rangle$  was used. The level scheme is shown in Fig. 4.9. The four states can be coupled by driving two off-resonant Raman beams (indicated by the arrows). Depending on the difference

<sup>19</sup>This discovery triggered the new research field of post-quantum cryptography, as many current cryptographic algorithms are based on the asymmetry of computational time between multiplying two large prime numbers and factorizing the resulting product. See for example [42].



**Fig. 4.9:** Level scheme of the two qubit system on which the CNOT operation was implemented. Two Raman beams (solid arrows) can couple any pair of a lower and an upper state, additionally  $|1\rangle|\uparrow\rangle$  can be coupled to an auxiliary level  $|\text{aux}\rangle$  (dashed arrows).

frequency  $\Delta$  between them, different states are coupled. For  $\Delta = \omega_0 + \omega_{\text{trap}}$  only  $|0\rangle|\downarrow\rangle$  and  $|1\rangle|\uparrow\rangle$  are coupled. Shining in with  $\Delta = \omega_0 - \omega_{\text{trap}}$  will couple  $|1\rangle|\downarrow\rangle$  and  $|0\rangle|\uparrow\rangle$ . A detuning of  $\Delta = \omega_0$  will couple the upper and lower levels without changing the motional quantum number.

The implementation of the CNOT operation with the help of the three lasers consists of a sequence of three Rabi pulses:

1. A  $\pi/2$ -pulse of the Raman lasers with  $\Delta = \omega_0$
2. A  $2\pi$ -pulse coupling  $|1\rangle|\uparrow\rangle$  and  $|\text{aux}\rangle$
3. A  $\pi/2$ -pulse of the Raman lasers with  $\Delta = \omega_0$  and a phase shift of  $\pi$  relative to the first pulse

To understand how this really defines a CNOT operation we go through the action on a wave function step by step. The Rabi cycle shown in Fig. 2.1 is of some help for illustration purposes. Assume that the system is initially in the state

$$|\Psi_{\text{init}}\rangle = |1\rangle|\uparrow\rangle.$$

In the first step this state is coupled to the lower lying  $|1\rangle|\downarrow\rangle$  by a  $\pi/2$ -pulse, taking it to the superposition state<sup>20</sup>

$$|\Psi_1\rangle = \frac{1}{\sqrt{2}}(|1\rangle|\uparrow\rangle - i|1\rangle|\downarrow\rangle)$$

The second step consists of applying a  $2\pi$ -pulse on the auxiliary transition, by which only the  $|1\rangle|\uparrow\rangle$  part of the wavefunction will receive a minus sign, resulting in

$$|\Psi_2\rangle = -\frac{1}{\sqrt{2}}(|1\rangle|\uparrow\rangle + i|1\rangle|\downarrow\rangle).$$

The last step is again a  $\pi/2$ -pulse on  $\omega_0$  but shifted by  $\pi$  relative to the first one, which corresponds to a counterclockwise step in Fig. 2.1, thus yielding

$$|\Psi_{\text{final}}\rangle = -i|1\rangle|\downarrow\rangle$$

<sup>20</sup>Following the nomenclature in Fig. 2.1 we identify  $|1\rangle|\uparrow\rangle$  with  $|e\rangle$  and  $|1\rangle|\downarrow\rangle$  with  $|g\rangle$ .

which will be detected as  $|1\rangle|\downarrow\rangle$ .<sup>21</sup> We see that in three steps the target qubit has been flipped as expected for a control qubit of  $|1\rangle$ . The other possible cases work accordingly, with any state with control qubit  $|0\rangle$  being unaffected by the sign change in step 2 and thus not experiencing a qubit flip.

The experimental results for prepared states before and after CNOT operation are shown in Fig 4.8b. It can be seen that the operation qualitatively works as expected, interchanging the two states with control qubit  $|1\rangle$ . Yet the fidelity is smaller than one due to effects of imperfect cooling or decoherence. However the advantage of using ions as qubits is that it can easily be scaled, for example by storing a larger number of ions in a linear Paul trap using each of them to store two qubits of information. An example of such an approach is the planned Q20:20 machine in Oxford, consisting of twenty times twenty trapped ions that are optically linked to each other[43].

---

<sup>21</sup>The detection scheme of Wineland et al. in this case does explicitly not yield the full phase information of the operation.

## 5 Conclusion

Having now visited some of the experiments that Serge Haroche and David Wineland realized, the similarities between their fields of research have become even more clear. Theoretically single trapped ions and atoms in cavities can be treated equivalently by applying the Jaynes-Cummings Hamiltonian and the method of Fock states to describe either the photon number or the quantum number of motion. Also experimentally we see that to observe the desired quantum mechanical effects both of them put huge effort into the isolation of single quanta.

To this day Serge Haroche continues to do research in the field of cavity quantum electrodynamics, some of his current interests being non-local quantum states and the quantum engineering of Rydberg states, at École Normale Supérieure in Paris. Also David Wineland continues to be the leader of the ion storage group at NIST working on high precision time standards and quantum information processing, this being another interesting parallel between the two.

Especially in association with prestigious prizes, the work of the laureates is often depicted as the sole performance of extraordinary individuals. At least in the case of Serge Haroche and David Wineland this is not true, as they both pointed out in their Nobel lectures [34, 44]. Both of them had important colleagues some of which spent more than forty years in the laboratories with them and contributed important ideas to their work. Both of them have been lucky to work along with great scientists of current and preceding generations from their very first days of research. Further it is important to realize what role technological progress played. Without the invention of tunable lasers, pulsed lasers, ion traps or superconducting materials, none of the experiments would have been possible. To put it in the words of Serge Haroche:

“On the professional side, I have had the luck to embark in a field - atomic physics and quantum optics - which has undergone fantastic developments over this period of time, improving by many orders of magnitudes the sensitivity of experiments and the precision of measurements. Thanks to advances in laser technology, new domains have been explored, in ultra-low temperature physics or in the study of ultrafast phenomena for instance, that we could not even imagine at the time I was working for my PhD. I did not work myself in many of these fields, but I witnessed these developments as a member of a very active and imaginative community of physicists, sharing the excitement and the bewilderment brought about by all these spectacular advances.” [10]

This said we end the term paper with the remark that both of the laureates have left an impressive lifework that was and is definitely worth the study.

## References

1. Gleyzes, S., Kuhr, S., Guerlin, C., Bernu, J., Deleglise, S., Hoff, U. B., Brune, M., Raimond, J.-M. & Haroche, S. Quantum jumps of light recording the birth and death of a photon in a cavity. *Nature* **446**, 297–300 (2007).
2. Brune, M., Haroche, S., Raimond, J., Davidovich, L. & Zagury, N. Manipulation of photons in a cavity by dispersive atom-field coupling: Quantum-nondemolition measurements and generation of “Schrödinger cat” states. *Physical Review A* **45**, 5193 (1992).
3. Monroe, C., Meekhof, D., King, B. & Wineland, D. J. A “Schrodinger cat” superposition state of an atom. *Science* **272**, 1131 (1996).
4. Rauschenbeutel, A., Nogues, G., Osnaghi, S., Bertet, P., Brune, M., Raimond, J.-M. & Haroche, S. Step-by-step engineered multiparticle entanglement. *Science* **288**, 2024–2028 (2000).
5. Sackett, C., Kielpinski, D., King, B., Langer, C., Meyer, V., Myatt, C., Rowe, M., Turchette, Q., Itano, W., Wineland, D., *et al.* Experimental entanglement of four particles. *Nature* **404**, 256–259 (2000).
6. Meekhof, D., Monroe, C., King, B., Itano, W. & Wineland, D. Generation of non-classical motional states of a trapped atom. *Physical Review Letters* **76**, 1796 (1996).
7. Deleglise, S., Dotsenko, I., Sayrin, C., Bernu, J., Brune, M., Raimond, J.-M. & Haroche, S. Reconstruction of non-classical cavity field states with snapshots of their decoherence. *Nature* **455**, 510–514 (2008).
8. Jaynes, E. T. & Cummings, F. W. Comparison of quantum and semiclassical radiation theories with application to the beam maser. *Proceedings of the IEEE* **51**, 89–109 (1963).
9. Gerry, C. & Knight, P. *Introductory quantum optics* (Cambridge university press, 2005).
10. Haroche, S. *Biographical* <[http://www.nobelprize.org/nobel\\_prizes/physics/laureates/2012/haroche-bio.html](http://www.nobelprize.org/nobel_prizes/physics/laureates/2012/haroche-bio.html)> (2012).
11. Haroche, S., Paisner, J. & Schawlow, A. Hyperfine quantum beats observed in Cs vapor under pulsed dye laser excitation. *Physical Review Letters* **30**, 948 (1973).
12. Goy, P., Raimond, J., Gross, M. & Haroche, S. Observation of cavity-enhanced single-atom spontaneous emission. *Physical review letters* **50**, 1903 (1983).

13. Brune, M., Haroche, S., Lefevre, V., Raimond, J. & Zagury, N. Quantum non-demolition measurement of small photon numbers by Rydberg-atom phase-sensitive detection. *Physical review letters* **65**, 976 (1990).
14. Nogues, G., Rauschenbeutel, A., Osnaghi, S., Brune, M., Raimond, J. & Haroche, S. Seeing a single photon without destroying it. *Nature* **400**, 239–242 (1999).
15. Jhe, W., Anderson, A., Hinds, E., Meschede, D., Moi, L. & Haroche, S. Suppression of spontaneous decay at optical frequencies: Test of vacuum-field anisotropy in confined space. *Physical review letters* **58**, 666 (1987).
16. Haroche, S. *Biographie* <<https://www.college-de-france.fr/site/serge-haroche/>> (2016).
17. Scully, M. O. & Zubairy, M. S. *Quantum optics* 16–19 (Cambridge university press, 1997).
18. Kuhr, S., Gleyzes, S., Guerlin, C., Bernu, J., Hoff, U. B., Deléglise, S., Osnaghi, S., Brune, M., Raimond, J.-M., Haroche, S., et al. Ultrahigh finesse Fabry-Pérot superconducting resonator. *arXiv preprint quant-ph/0612138* (2006).
19. Gleyzes, S., Kuhr, S., Guerlin, C., Bernu, J., Deleglise, S., Hoff, U. B., Brune, M., Raimond, J.-M. & Haroche, S. Quantum jumps of light recording the birth and death of a photon in a cavity. *Nature* **446**, 297–300 (2007).
20. Guerlin, C., Bernu, J., Deleglise, S., Sayrin, C., Gleyzes, S., Kuhr, S., Brune, M., Raimond, J.-M. & Haroche, S. Progressive field-state collapse and quantum non-demolition photon counting. *Nature* **448**, 889–893 (2007).
21. Wineland, D. *Biographical* <[http://www.nobelprize.org/nobel\\_prizes/physics/laureates/2012/wineland-bio.html](http://www.nobelprize.org/nobel_prizes/physics/laureates/2012/wineland-bio.html)> (2012).
22. Wineland, D. J. & Ramsey, N. Atomic deuterium maser. *Physical Review A* **5**, 821 (1972).
23. Wineland, D., Ekstrom, P. & Dehmelt, H. Monoelectron oscillator. *Physical review letters* **31**, 1279 (1973).
24. Dehmelt, H. & Wineland, D. *Bulletin of the American Physical Society* **20** (1975).
25. Wineland, D. J., Drullinger, R. E. & Walls, F. L. Radiation-pressure cooling of bound resonant absorbers. *Physical Review Letters* **40**, 1639 (1978).
26. Neuhauser, W., Hohenstatt, M., Toschek, P. & Dehmelt, H. Optical-sideband cooling of visible atom cloud confined in parabolic well. *Physical Review Letters* **41**, 233 (1978).
27. Wineland, D. & Itano, W. M. Spectroscopy of a single Mg+ ion. *Physics Letters A* **82**, 75–78 (1981).

28. Bergquist, J., Hulet, R. G., Itano, W. M. & Wineland, D. Observation of quantum jumps in a single atom. *Physical review letters* **57**, 1699 (1986).
29. Diedrich, F., Bergquist, J., Itano, W. M. & Wineland, D. Laser cooling to the zero-point energy of motion. *Physical Review Letters* **62**, 403 (1989).
30. Monroe, C., Meekhof, D., King, B., Itano, W. & Wineland, D. Demonstration of a fundamental quantum logic gate. *Physical review letters* **75**, 4714 (1995).
31. Leibfried, y., Blatt, R., Monroe, C. & Wineland, D. Quantum dynamics of single trapped ions. *Reviews of Modern Physics* **75**, 281 (2003).
32. Hänsch, T. W. & Schawlow, A. L. Cooling of gases by laser radiation. *Optics Communications* **13**, 68–69 (1975).
33. Mudrich, M. *Lecture Notes in Atomic and Molecular Physics* 2015.
34. Wineland, D. Nobel Lecture: Superposition, Entanglement and Raising Schrödinger's cat (2012).
35. Nagourney, W., Sandberg, J. & Dehmelt, H. Shelved optical electron amplifier: Observation of quantum jumps. *Physical Review Letters* **56**, 2797 (1986).
36. Sauter, T., Neuhauser, W., Blatt, R. & Toschek, P. Observation of quantum jumps. *Physical review letters* **57**, 1696 (1986).
37. Gabrielse, G., Peil, S., Odom, B. & D'Urso, B. *QND observation of quantum jumps between Fock states: a one-electron cyclotron oscillator at 70 mK to 4.2 K* in *Quantum Electronics and Laser Science Conference, 1999. QELS'99. Technical Digest. Summaries of Papers Presented at the* (1992), 19–20.
38. Basché, T., Kummer, S. & Bräuchle, C. Direct spectroscopic observation of quantum jumps of a single molecule. *Nature* **373**, 132–134 (1995).
39. Bergquist, J., Itano, W. M. & Wineland, D. Recoilless optical absorption and Doppler sidebands of a single trapped ion. *Physical Review A* **36**, 428 (1987).
40. Feynman, R. P. Simulating physics with computers. *International journal of theoretical physics* **21**, 467–488 (1982).
41. Shor, P. W. *Algorithms for quantum computation: Discrete logarithms and factoring* in *Foundations of Computer Science, 1994 Proceedings., 35th Annual Symposium on* (1994), 124–134.
42. Bernstein, D. J., Buchmann, J. & Dahmen, E. *Post-quantum cryptography* (Springer Science & Business Media, 2009).
43. Oxford to lead UK quantum computer drive <<http://www.ox.ac.uk/news/2014-11-26-oxford-lead-uk-quantum-computer-drive>> (2016).

44. Haroche, S. Controlling Photons in a Box and Exploring the Quantum to Classical Boundary (2012).